arXiv:0803.3174v1 [cond-mat.supr-con] 21 Mar 2008

Induced Triplet Pairing in clean s-wave Superconductor/Ferromagnet layered structures

Klaus Halterman,[1,*] Oriol T. Valls,[2,†] and Paul H. Barsic[2,‡]

[1]*Physics and Computational Sciences, Research and Engineering Sciences Department, Naval Air Warfare Center, China Lake, California 93555*

[2]*School of Physics and Astronomy, University of Minnesota, Minneapolis, Minnesota 55455*

(Dated: March 21, 2008)

We study induced triplet pairing correlations in clean ferromagnet/superconductor/ferromagnet heterostructures. The pairing state in the superconductor is the conventional singlet s-wave, and the angle α between the magnetizations of the two ferromagnetic layers is arbitrary. We use a numerical fully self-consistent solution of the microscopic equations and obtain the time-dependent triplet correlations via the Heisenberg equations of motion. We find that in addition to the usual singlet correlations, triplet correlations, odd in time as required by the Pauli principle, are induced in both the ferromagnets and the superconductor. These time-dependent correlations are largest at times of order of the inverse of the Debye cutoff frequency, ω_D, and we find that within that time scale they are often spatially very long ranged. We discuss the behavior of the characteristic penetration lengths that describe these triplet correlations. We also find that the ferromagnets can locally magnetize the superconductor near the interface, and that the local magnetization then undergoes strongly damped oscillations. The local density of states exhibits a variety of energy signatures, which we discuss, as a function of ferromagnetic strength and α.

PACS numbers: 74.45.+c, 74.25.Bt, 74.78.Fk

I. INTRODUCTION

Triplet Cooper pairing is no new phenomenon: it has long been recognized to be responsible for superfluidity[1] in ^{3}He as well as for superconductivity in some electronic materials. This occurs when the pairing interaction is in a partial wave with odd ℓ. However, recent observations have raised the possibility of induced triplet pairing correlations in s-wave superconductors. It is a matter of elementary physics that the Cooper pair wavefunction must be antisymmetric under exchange of the two electrons to satisfy the Pauli principle. For spatially symmetric s-wave superconductors with decoupled spatial and spin degrees of freedom, the spin singlet pair is the only possible antisymmetric state of an electron pair. Triplet pairing states on the other hand, where the spin state is symmetric, are obviously allowed when the pairing is spatially antisymmetric, such as in p-wave superconductors. Triplet states in systems with s-wave pairing, even in momentum or coordinate space, would naively appear to violate the Pauli principle. However, many years ago Berezinskii proposed[2] a triplet state in superfluid ^{3}He, which involved spatially symmetric correlations. Berezinskii's triplet pairing correlations, involving different-time pairing, did not violate the Pauli principle by virtue of being odd in time, thus allowing a triplet state in a system with s-wave interactions. While such a state did not turn out to be appropriate to describe superfluidity in ^{3}He, its consideration has led the way to the study of cases where some sort of time-reversal symmetry breaking mechanism may allow an odd time triplet state to be induced in systems with spatially symmetric interactions.

Interest in exotic triplet pairing arises from many quarters. In the case of two component cold atomic gases[3] with short-range s-wave interactions, in which the two species have the same mass but different chemical potentials, it may be possible to induce a triplet pairing that breaks time reversal symmetry. In electronic materials, an important issue is the possible existence of a long range proximity effect in Superconductor/Ferromagnet (SF) heterostructures. Interest in these heterostructures arises in turn from their possible[4] applications. Of particular interest is that the thermodynamic and transport properties of FSF trilayers are found to depend strongly on the relative orientation of the magnetization in the two F layers.[5,6,7,8] This rather well-understood[9,10,11,12] fact makes these structures candidates as spin valves.

There have been no unambiguous observations of induced triplet correlations in SF structures involving s-wave superconductors. However, there have been some enticing experimental hints in the form of long ranged proximity induced superconducting behavior in SF multilayers with strong exchange fields. The observed effects are over length scales much larger than those of the usual SF proximity effect and more like the much longer length scales associated with the standard proximity effect between a superconductor and a normal nonmagnetic metal. These observations include measurements in superlattices[13] with ferromagnetic spacers and SQUIDs[14] with ferromagnetic interlayers. Superconducting characteristics, such as a critical temperature and enhanced sub-gap conductance, have been observed in point contact conductance measurements on s-wave superconductor/half metallic systems.[15] Perhaps most compelling is the observation of a Josephson current through a strong almost half-metallic, ferromagnet.[16] All of these experiments indicate long range superconducting correlations that are not destroyed by a strong exchange field: a

triplet state would obviously be consistent with these experiments. To fully understand the behavior of these systems, further studies involving, for example, quantities sensitive to the gap such as the local density of states (local DOS), are needed. Until both better theoretical models and more varied experimental observations are made available, one cannot conclusively say that there is indeed an induced triplet state in these systems, but at this point the facts fit this explanation and no better one has been proposed.[17]

Many theoretical studies agree that it is possible to induce this exotic state in certain SF systems[17,18,19,20,21,22,23,24,25,26,27,28,29] (perhaps even in the nonmagnetic[30] case) with ordinary singlet pairing in S. Some studies use an SFF′S arrangement in which the F and F′ layers have different magnetization orientations. Others assume that a domain structure in a single F layer is responsible for the symmetry breaking. Yet others assume an FSF system with different in-plane magnetization orientations in the F layers. Whatever the mechanism for the symmetry breaking, such arrangements can induce, via proximity effects, triplet correlations of different kinds. Recently it was shown that a Josephson supercurrent can exist in a half metal by virtue of equal spin triplet pairs and spin flip scattering events at the interfaces.[28] To understand and probe the underlying triplet state, investigations have been done on conductance spectra in simpler FS structures[31] with arbitrary magnetization alignment and with spin active interfaces, as well as in diffusive[29] SF junctions, through characterizing the possible superconductor symmetry classes consistent with Pauli's principle. With the exception of our early work[18] on SFS trilayers and some recent work on SFS Josephson junctions,[28] the studies above are done in the dirty limit through linearized Usadel-type or other quasiclassical equations. The disadvantage of a quasiclassical approach is that it is unsuitable for magnets with an exchange field on the order of the Fermi energy. Thus, it cannot properly model a strong ferromagnet, and it does not allow for atomic scale oscillations in the pair amplitude. A good quantitative explanation requires a self-consistent treatment of a fully microscopic model. Thus, as pointed out in a recent review,[27] the very existence of triplet correlations in clean FS structures was until very recently generally doubted, and these doubts have only very recently[18] been dispelled.

In this paper we explore the phenomenon of induced triplet correlations, odd in time, of clean FSF structures, where S is an ordinary s-wave superconductor and the magnetizations in the two F layers are rotated by an arbitrary angle α. We assume strong ferromagnets (up to the half-metallic limit), and smooth, sharp interfaces. In this geometry, triplet correlations with total spin projection $m = 0$ on the axis of quantization of the Cooper pairs are in general possible and, when the relative magnetizations (which we assume as usual are both parallel to the interfaces) are not aligned, triplet components with $m = \pm 1$ are allowed also. To satisfy the Pauli principle, these spatially symmetric triplet pairing correlations must be odd in frequency or time.[2] That such correlations are allowed, does not mean that they must exist, nor that they must exist over an extended spatial range. We find, however, via a fully self-consistent solution to the microscopic Bogoliubov de-Gennes[32] (BdG) equations that such correlations do indeed exist, and that the penetration depth associated with them can be very long. Our use of the BdG equations allows us to study strong ferromagnets. Self-consistency is fundamental: non-self-consistent solutions are found to violate the Pauli principle. Thus, the time consuming step of calculating fully self-consistent solutions is necessary to properly model the proximity effects which allow for the mixing of superconducting and ferromagnetic orderings that causes these induced correlations.

In Sec. II of this paper, we discuss the basic equations and our method for numerical self-consistent solution. There, the extraction of the all-important time dependence via solution of the Heisenberg equations of motion for the relevant operators is explained in detail. Expressions for all of the time-dependent triplet correlations are also derived. The equations for the local density of states (local DOS) and the local magnetic moment (which we use to discuss the reverse proximity effect, that is, the penetration of the magnetism into the superconductor) are also presented. In the next section (Sec. III) we begin by presenting an extensive discussion of the triplet correlations as a function of position, α, and magnet strength. The appropriate penetration depths are extracted and discussed. Results for the DOS, the magnetic moment and the temperature dependence of both triplet and ordinary singlet correlations are also given. Finally, in Sec. IV, a brief conclusion and summary is given.

II. METHODS

The geometry we consider consists of a planar FSF junction as depicted in Fig. 1. The thickness of the superconducting layer is d_S and the F layers have thicknesses d_{F_1} and d_{F_2}. The system is assumed to be infinite in the plane perpendicular to the layers, which we label as our $x - z$ plane. The magnetizations of the F layers, which are in this plane, form an angle $\pm\alpha/2$ with the z axis, which is that of the direction of quantization of the spins.

Our starting point is the Bogoliubov de-Gennes (BdG) equations[32] for the system under consideration. The derivation of the BdG equations for the case of interest requires some care with the conventions for all operator phase factors, which are not universally agreed upon in the literature, and which may give rise to different signs in some of the equations below. We write the effective BCS Hamiltonian, $\mathcal{H}_{\rm eff}$, as

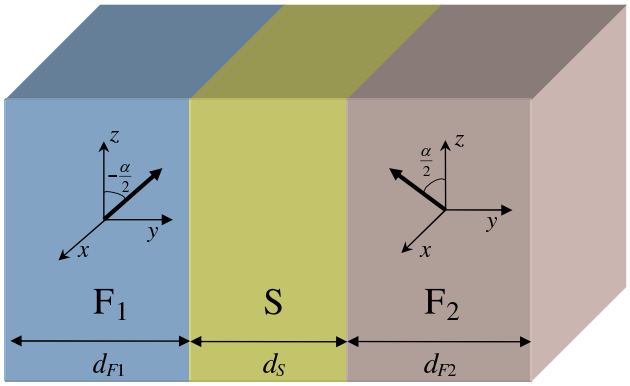

FIG. 1: (Color online) Schematic of the FSF junction. The y axis is normal to the interfaces. The left ferromagnet layer denoted F_1 has a magnetization oriented at an angle $-\alpha/2$ in the $x-z$ plane, while the other magnet F_2, has a magnetization orientation at an angle $\alpha/2$ in the $x-z$ plane. All layer widths are labeled.

$$\mathcal{H}_{\rm eff} = \int d^3r \Big\{ \sum_\alpha \psi^\dagger_\alpha(\mathbf{r}) \mathcal{H}_{\rm e} \psi_\alpha(\mathbf{r}) + \frac{1}{2}[\sum_{\alpha,\beta} (i\sigma_y)_{\alpha\beta} \Delta(\mathbf{r}) \psi^\dagger_\alpha(\mathbf{r}) \psi^\dagger_\beta(\mathbf{r}) + \text{h.c.}] - \sum_{\alpha,\beta} \psi^\dagger_\alpha(\mathbf{r}) (\mathbf{h}\cdot\boldsymbol{\sigma})_{\alpha\beta} \psi_\beta(\mathbf{r}) \Big\}, \tag{2.1}$$

where $\mathcal{H}_{\rm e} = -1/(2m)\boldsymbol{\nabla}^2 - E_F + U(\mathbf{r})$, $\boldsymbol{\sigma}$ are the set of Pauli matrices, spin is denoted by Greek indices, and as usual, we represent the magnetism of the F layers by an effective exchange Stoner energy $\mathbf{h}(\mathbf{r})$ which will in general have components in both the transverse (x,z) directions. The spin independent scattering potential is denoted $U(\mathbf{r})$, and $\Delta(\mathbf{r})$ is the usual pair potential.

To diagonalize the effective Hamiltonian, the field operators $\psi^\dagger_\alpha$ and ψ_α are expanded by means of a Bogoliubov transformation, which, for our phase convention, we write[33] as:

$$\psi_\uparrow(\mathbf{r}) = \sum_n \left(u_{n\uparrow}(\mathbf{r}) \gamma_n - v_{n\uparrow}(\mathbf{r}) \gamma^\dagger_n \right), \tag{2.2a}$$

$$\psi_\downarrow(\mathbf{r}) = \sum_n \left(u_{n\downarrow}(\mathbf{r}) \gamma_n + v_{n\downarrow}(\mathbf{r}) \gamma^\dagger_n \right), \tag{2.2b}$$

where $u_{n\alpha}$ and $v_{n\alpha}$ are the quasiparticle and quasihole amplitudes, and γ_n and $\gamma^\dagger_n$ are the Bogoliubov quasiparticle annihilation and creation operators, respectively.

We require that the transformations in Eqs. (2.2) diagonalize $\mathcal{H}_{\rm eff}$,

$$[\mathcal{H}_{\rm eff}, \gamma_n] = -\epsilon_n \gamma_n, \tag{2.3a}$$

$$[\mathcal{H}_{\rm eff}, \gamma^\dagger_n] = \epsilon_n \gamma^\dagger_n. \tag{2.3b}$$

One can also take the commutator $[\psi_\alpha(\mathbf{r}), \mathcal{H}_{\rm eff}]$. With the magnetizations in the $x-z$ plane as explained above, this gives the following,

$$[\psi_\uparrow(\mathbf{r}), \mathcal{H}_{\rm eff}] = (\mathcal{H}_{\rm e} - h_z)\psi_\uparrow(\mathbf{r}) - h_x \psi_\downarrow(\mathbf{r}) + \Delta(\mathbf{r})\psi^\dagger_\downarrow(\mathbf{r}), \tag{2.4a}$$

$$[\psi_\downarrow(\mathbf{r}), \mathcal{H}_{\rm eff}] = (\mathcal{H}_{\rm e} + h_z)\psi_\downarrow(\mathbf{r}) - h_x \psi_\uparrow(\mathbf{r}) - \Delta(\mathbf{r})\psi^\dagger_\uparrow(\mathbf{r}). \tag{2.4b}$$

Inserting (2.2) into (2.4) and using Eqs. (2.3) yields the general spin-dependent BdG equations,

$$\begin{pmatrix} \mathcal{H}_0 - h_z(y) & -h_x(y) & 0 & \Delta(y) \\ -h_x(y) & \mathcal{H}_0 + h_z(y) & \Delta(y) & 0 \\ 0 & \Delta(y) & -(\mathcal{H}_0 - h_z(y)) & -h_x(y) \\ \Delta(y) & 0 & -h_x(y) & -(\mathcal{H}_0 + h_z(y)) \end{pmatrix} \begin{pmatrix} u_{n\uparrow}(y) \\ u_{n\downarrow}(y) \\ v_{n\uparrow}(y) \\ v_{n\downarrow}(y) \end{pmatrix} = \epsilon_n \begin{pmatrix} u_{n\uparrow}(y) \\ u_{n\downarrow}(y) \\ v_{n\uparrow}(y) \\ v_{n\downarrow}(y) \end{pmatrix}, \tag{2.5}$$

where the single particle Hamiltonian $\mathcal{H}_0$ is defined as,

$$\mathcal{H}_0 \equiv \frac{\widehat{p}_y^2}{2m} + \varepsilon_\perp - E_F + U(y). \tag{2.6}$$

A plane wave factor $e^{i\mathbf{k}_\perp \cdot \mathbf{r}}$ has been canceled in both

sides of Eq. (2.5). The longitudinal momentum operator, $\widehat{p}_y$, is given by, $\widehat{p}_y = -i\partial/\partial y$, $\varepsilon_\perp$ is the kinetic energy of the transverse modes, $\Delta(y)$ is the self-consistent pair potential, and $U(y)$ is a scalar potential representing interface scattering characterized by a delta function of strength H_B. The ferromagnetic exchange field $\mathbf{h}(y) = (h_x(y), 0, h_z(y))$, vanishes in the S layers. We have $h_x(y) = h_0 \sin(-\alpha/2)$ and $h_z(y) = h_0 \cos(-\alpha/2)$ in the F_1 layer, where h_0 is the magnitude of the exchange field, while in F_2, $h_x(y) = h_0 \sin(\alpha/2)$, and $h_z(y) = h_0 \cos(\alpha/2)$. We refer to Fig. 1 for details. The dimensionless parameter $I \equiv h_0/E_F$ conveniently characterizes the strength of the magnetism. One thus has $I = 1$ in the half metallic limit. If we take $\alpha = 0$ or π, i.e. the magnetizations of both layers lie along the same direction, or if there is only one F layer, then $h_x = 0$ and we recover the simpler form of the BdG equations used[9,34] in other contexts. We can find the quasiparticle amplitudes on a different quantization axis in the $x - z$ plane forming an angle α' with z, by performing a spin rotation $\Phi_n \to \widehat{U}(\alpha')\Phi_n$ with,

$$\widehat{U}(\alpha') = \cos(\alpha'/2)\hat{1} \otimes \hat{1} - i \sin(\alpha'/2)\rho_z \otimes \sigma_y, \qquad (2.7)$$

where we have introduced $\boldsymbol{\rho}$ as a set of Pauli-like matrices in particle-hole space. It is convenient to use the matrices $\boldsymbol{\rho}$ in conjunction with the ordinary Pauli matrices $\boldsymbol{\sigma}$ in spin space to rewrite Eqs. (2.5) in the more compact but perhaps less transparent way:

$$\left[\rho_z \otimes \left(\mathcal{H}_0 \hat{\mathbf{1}} - h_z \sigma_z\right) + \left(\Delta(y)\rho_x - h_x \hat{\mathbf{1}}\right) \otimes \sigma_x\right] \Phi_n = \epsilon_n \Phi_n, \qquad (2.8)$$

where $\Phi_n \equiv (u_{n\uparrow}(y), u_{n\downarrow}(y), v_{n\uparrow}(y), v_{n\downarrow}(y))^{\mathrm{T}}$, with the superindex denoting transposition.

The usual self consistency condition relates the spectrum obtained from Eq. (2.5) to the inhomogeneous pair potential $\Delta(y)$ by an appropriate sum over states:

$$\Delta(y) = \frac{g(y)}{2} {\sum_n}' \left[u_n^\uparrow(y) v_n^\downarrow(y) + u_n^\downarrow(y) v_n^\uparrow(y)\right] \tanh(\epsilon_n/2T), \qquad (2.9)$$

where the prime on the sum indicates that only those positive energy states with energy less than the pairing interaction energy cutoff, ω_D, are included, and T is the temperature. The function $g(y)$ vanishes in the F layers while in the S layers it takes the value of the usual BCS *singlet* coupling constant in the S material.

With an appropriate choice of basis,[34,35] Eqs. (2.5) can be cast into a finite $4N \times 4N$ dimensional matrix eigenvalue system. In dimensionless form, it reads,

$$\begin{bmatrix} H_0 - H_z & -H_x & 0 & D \\ -H_x & H_0 + H_z & D & 0 \\ 0 & D & -(H_0 - H_z) & -H_x \\ D & 0 & -H_x & -(H_0 + H_z) \end{bmatrix} \Psi_n = \widetilde{\epsilon}_n \Psi_n, \qquad (2.10)$$

where $\widetilde{\epsilon}_n \equiv \epsilon_n/E_F$, and Ψ_n, the transpose of

$$\Psi_n^T = (u_{n1}^\uparrow, \ldots, u_{nN}^\uparrow, u_{n1}^\downarrow, \ldots, u_{nN}^\downarrow, v_{n1}^\uparrow, \ldots, v_{nN}^\uparrow, v_{n1}^\downarrow, \ldots, v_{nN}^\downarrow), \qquad (2.11)$$

contains the expansion coefficients associated with the set of orthonormal basis functions. We write $u_n^\alpha(z) = \sqrt{2/d} \sum_{q=1}^N u_{nq}^\alpha \sin(q\pi z/d)$, and $v_n^\alpha(z) = \sqrt{2/d} \sum_{q=1}^N v_{nq}^\alpha \sin(q\pi z/d)$, for $\alpha = \uparrow, \downarrow$. The necessary matrix elements analogous to Eqn. (2.5) for different π junction geometries and for strictly collinear magnetization orientations have been calculated in previous work.[34,35] The situation is more complicated for the case of a FSF trilayer considered

here, with the magnetization angles of the two F layers forming an angle α. The matrix elements are then written as,

$$(H_0)_{mn} = \left[\left(\frac{m\pi}{k_F d}\right)^2 + \frac{\varepsilon_\perp}{E_F} - 1\right]\delta_{mn} + Z_B[\mathcal{U}_{m-n}(d_{F1}) + \mathcal{U}_{m-n}(d_{F1}+d_S) - \mathcal{U}_{m+n}(d_{F1}) - \mathcal{U}_{m+n}(d_{F1}+d_S)], \tag{2.12a}$$

$$(H_z)_{mn} = \frac{h_0}{E_F}\cos(\alpha/2)\big[\mathcal{K}_{m-n}(d_{F1}) - \mathcal{K}_{m+n}(d_{F1}) + \mathcal{K}_{m+n}(d_{F1}+d_S) - \mathcal{K}_{m-n}(d_{F1}+d_S)\big], \quad m \neq n, \tag{2.12b}$$

$$= \frac{h_0}{E_F}\cos(\alpha/2)\left[\frac{d_{F1}+d_{F2}}{d} + \mathcal{K}_{2m}(d_{F1}+d_S) - \mathcal{K}_{2m}(d_{F1})\right], \quad m = n, \tag{2.12c}$$

$$(H_x)_{mn} = \frac{h_0}{E_F}\sin(\alpha/2)\big[\mathcal{K}_{m+n}(d_{F1}) - \mathcal{K}_{m-n}(d_{F1}) + \mathcal{K}_{m+n}(d_{F1}+d_S) - \mathcal{K}_{m-n}(d_{F1}+d_S)\big], \quad m \neq n, \tag{2.12d}$$

$$= \frac{h_0}{E_F}\sin(\alpha/2)\left[\frac{d_{F2}-d_{F1}}{d} + \mathcal{K}_{2m}(d_{F1}+d_S) + \mathcal{K}_{2m}(d_{F1})\right], m = n, \tag{2.12e}$$

$$(D)_{mn} = \frac{2}{E_F d}\int_{d_{F1}}^{d_{F1}+d_S} dy \sin\left[\frac{m\pi y}{d}\right]\Delta(y)\sin\left[\frac{n\pi y}{d}\right], \tag{2.12f}$$

where $Z_B \equiv 2H_B/(k_F d)$ is a convenient dimensionless measure of interfacial scattering. We have also defined:

$$\mathcal{K}_n(y) \equiv \frac{\sin\left(\frac{n\pi y}{d}\right)}{n\pi}, \quad \mathcal{U}_n(y) \equiv \cos\left(\frac{n\pi y}{d}\right). \tag{2.13}$$

We now consider the appropriate quantities that characterize the induced triplet correlations. To do this, we define the following *triplet* pair amplitude functions in terms of the field operators,

$$\mathbf{f_0}(\mathbf{r},t) = \frac{1}{2}[\langle\psi_\uparrow(\mathbf{r},t)\psi_\downarrow(\mathbf{r},0)\rangle + \langle\psi_\downarrow(\mathbf{r},t)\psi_\uparrow(\mathbf{r},0)\rangle], \tag{2.14a}$$

$$\mathbf{f_1}(\mathbf{r},t) = \frac{1}{2}[\langle\psi_\uparrow(\mathbf{r},t)\psi_\uparrow(\mathbf{r},0)\rangle - \langle\psi_\downarrow(\mathbf{r},t)\psi_\downarrow(\mathbf{r},0)\rangle]. \tag{2.14b}$$

We will later demonstrate that these amplitudes vanish at $t = 0$, as required by the Pauli principle.

To make use of these expressions, it is most convenient to use the Heisenberg picture. Thus we write ψ_ς in the Heisenberg representation:

$$\psi_\varsigma(t) = e^{(i\mathcal{H}_{\rm eff}t)}\psi_\varsigma e^{(-i\mathcal{H}_{\rm eff}t)}. \tag{2.15}$$

To put this in terms of the quasiparticle amplitudes, we apply Eqns. (2.2) and the transformation Eqns. (2.3). We can then immediately write down the Heisenberg equations of motion for the γ's as

$$i\frac{\partial\gamma_n}{\partial t} = [\gamma_n, \mathcal{H}_{\rm eff}] \tag{2.16}$$

and

$$i\frac{\partial\gamma_n^\dagger}{\partial t} = [\gamma_n^\dagger, \mathcal{H}_{\rm eff}]. \tag{2.17}$$

These equations of motion, given Eqns. (2.3), have the solutions $\gamma_n(t) = \gamma_n e^{-i\epsilon_n t}$ and $\gamma_n^\dagger(t) = \gamma_n^\dagger e^{i\epsilon_n t}$. When we substitute these results into the above equations for $\mathbf{f_0}$ and $\mathbf{f_1}$, taking into account Eqns. (2.2) we obtain:

$$\mathbf{f_0}(y,t) = \frac{1}{2}\sum_n [u_{n\uparrow}(y)v_{n\downarrow}(y) - u_{n\downarrow}(y)v_{n\uparrow}(y)]\zeta_n(t), \tag{2.18a}$$

$$\mathbf{f_1}(y,t) = -\frac{1}{2}\sum_n [u_{n\uparrow}(y)v_{n\uparrow}(y) + u_{n\downarrow}(y)v_{n\downarrow}(y)]\zeta_n(t), \tag{2.18b}$$

where $\zeta_n(t) \equiv \cos(\epsilon_n t) - i\sin(\epsilon_n t)\tanh(\epsilon_n/2T)$. The spatial dependence of the complex quantities $\mathbf{f_0}(y,t)$ and $\mathbf{f_1}(y,t)$ is, in our geometry, on the y coordinate only. They vanish identically at $t = 0$.

We will focus on in our study of the induced triplet correlations on the time dependent quantities $\mathbf{f_0}(y,t)$ and $\mathbf{f_1}(y,t)$. Their existence at $t > 0$ is allowed by the Pauli principle. It is also important to sort out when it is allowed by the spin symmetries: when the axis of quantization of the Cooper pairs is the only axis of quantization in the system (i.e., when $\alpha = 0$) then it is not hard to see that the total spin operator $\mathbf{S}$ of the Cooper pairs does not commute with the Hamiltonian. This is best seen directly from the matrix expression on the left side of Eqn. (2.5). On the other hand, S_z and the Hamiltonian do commute in this case. However, when α (and therefore h_x) is nonzero, then no component of $\mathbf{S}$ commutes with the effective Hamiltonian. From this spin symmetry argument it follows that the induced amplitude $\mathbf{f_1}(y,t)$ may exist (at finite times) only at nonzero α, while $\mathbf{f_0}(y,t)$ is allowed ant any α. For $\alpha = \pi$, when the magnetizations are antiparallel and along the x axis, no triplet amplitudes with nonzero component along that axis can exist.

The matrix $\widehat{U}(\alpha)$ in Eq. (2.7) can be used to verify this by performing the corresponding spin rotations. That the existence of certain quantities is consistent with all symmetry properties does not mean that these quantities will indeed be nonvanishing, and it certainly tells us nothing about the possible range and behavior in space and time of these amplitudes. To determine this requires detailed calculations.

Also of considerable interest in F/S structures is the reverse proximity effect: the leakage of magnetism out of the magnets and into the superconductor. This can be characterized by the local magnetization $\mathbf{m}(y)$. It is defined as,

$$\mathbf{m} = -\mu_B \langle \sum_\sigma \psi_\sigma^\dagger \boldsymbol{\sigma} \psi_\sigma \rangle, \tag{2.19}$$

where μ_B is the Bohr magneton. The vector $\mathbf{m}$ has two components in the FSF geometry discussed. Both components depend on y. They are:

$$m_z(y) = -\mu_B \sum_n \left\{ \left[|u_{n\uparrow}(y)|^2 - |u_{n\downarrow}(y)|^2 \right] f_n + \left[|v_{n\uparrow}(y)|^2 - |v_{n\downarrow}(y)|^2 \right] (1 - f_n) \right\}, \tag{2.20}$$

and

$$m_x(y) = -2\mu_B \sum_n \left\{ \left[u_{n\uparrow}(y) u_{n\downarrow}(y) \right] f_n + \left[v_{n\uparrow}(y) v_{n\downarrow}(y) \right] (1 - f_n) \right\}. \tag{2.21}$$

It is convenient to normalize these components to $-\mu_B(N_\uparrow + N_\downarrow)$, where $N_\uparrow = k_F^3(1+I)^{3/2}/(6\pi^2)$, and $N_\downarrow = k_F^3(1-I)^{3/2}/(6\pi^2)$.

The proximity effects can also be examined through the local DOS, $N(y,\epsilon)$, given by,

$$N(y,\epsilon) = -\sum_n \{ [u_{n\uparrow}^2(y) + u_{n\downarrow}^2(y)] f'(\epsilon - \epsilon_n) + [v_{n\uparrow}^2(y) + v_{n\downarrow}^2(y)] f'(\epsilon + \epsilon_n) \}, \tag{2.22}$$

where $f' = \partial f / \partial \epsilon$. We will be concerned mainly with the DOS normalized to the DOS of a bulk (unpolarized) normal metal, $D_N(0) = k_F^3/(2\pi^2 E_F)$.

III. RESULTS

In this section we present our results, obtained self consistently as explained above and in previous[18,34,35] work. We have assumed a coherence length $k_F\xi_0 = 100$. We will choose a geometry in which the layers are relatively thick: $k_F d_s \equiv D_S = 200$ (that is, two coherence lengths) and $D_{F_1} = D_{F_2} = 250$. These values ensure that the sample will be overall superconducting at temperatures up to about 1/3 of the transition temperature T_c, of a pure S bulk sample. This was not the case for the smaller values used in Ref. 18 where the condensation energy was quite small (see e.g. figure 6 in Ref. 35). This allows us to study the temperature dependence of the quantities involved over a broad range. The most important parameters are the angle α and the magnet strength I. We will vary α in its full range between 0 and π and give results for the values of I of 0.25, 0.5, and unity. No triplet amplitudes arise at $I = 0$ (when magnetism is absent). In the results presented we have $Z_B = 0$, when proximity effects are in general maximized.

In Fig. 2 we present comprehensive results for the real parts of $\mathbf{f_0}(y,t)$ and $\mathbf{f_1}(y,t)$, which we denote simply as $f_0(y,t)$ and $f_1(y,t)$ respectively. These are plotted in terms of the dimensionless variable $Y \equiv k_F y$. The amplitudes are normalized to the value of the usual singlet amplitude in a pure bulk S sample. The temperature is set to zero in this figure. In the main plots, half of the S region and a portion (three fifths) of the left (F_1) region are included. The corresponding portion on the F_2 side can be inferred from the geometry and symmetry considerations. Results are plotted at three values of I and at a number of finite times $\tau \equiv \omega_D t$ between 0.4 and 8 as indicated in the legends. We have verified that at $t = 0$ the computed triplet amplitudes vanish identically, in agreement with the Pauli principle. This is true, however, only when the calculation is performed to self-consistency: *non-self consistent results invariably violate the Pauli principle* near the interface. The results for f_0 are given at an angle $\alpha = 0$ while those for f_1 are at $\alpha = \pi/2$. At $\alpha = 0$, f_1 vanishes identically since the z component of the total spin is then a good quantum number. At $\alpha = \pi/2$, and short time scales, the spatial dependences of the two triplet components coincide, albeit with different signs in the two magnet regions, due to the magnetization vectors having equal projections on the x and z axes. At longer times, when the triplet amplitudes extend throughout the S layer and couple the two magnets, f_0 and f_1 deviate from one another. The insets in each panel amplify and clarify the region near the interfaces.

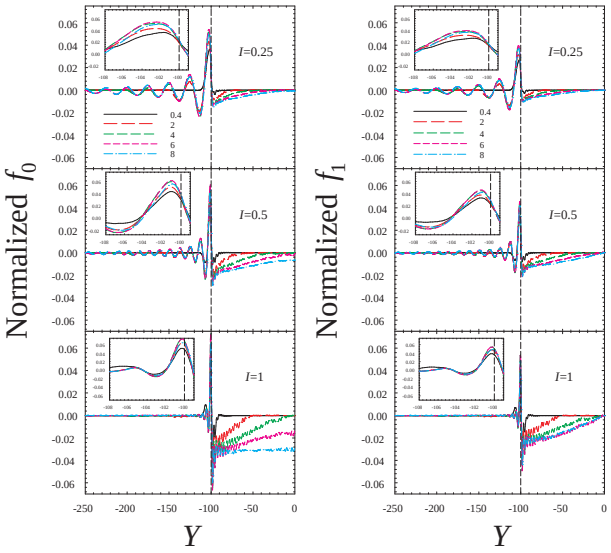

FIG. 2: The real parts, f_0 and f_1, of the triplet pair amplitudes $\mathbf{f_0}$ and $\mathbf{f_1}$ (Eqns. (2.18)), plotted as a function of position (in terms of $Y \equiv k_F y$) for three values of I at different times $\tau \equiv \omega_D t$ indicated in the legends of the top panels. These quantities are normalized to the value of the singlet pairing amplitude in a bulk S material. The main plots show half of the S region (right side of the vertical dashed line), and part of the F_1 region. The insets are blow-ups of the region near the interface. The angle α is zero in the left panel and $\pi/2$ in the right panel.

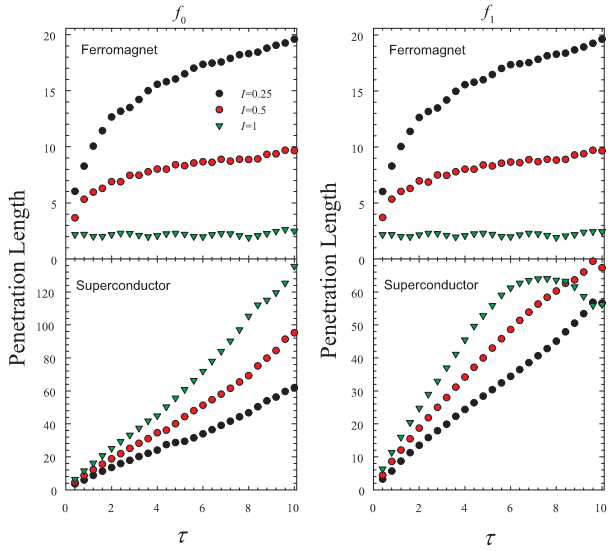

FIG. 3: Penetration depths for the triplet amplitudes (see Eq. (3.1)), plotted as a function of τ, as calculated from f_0 and f_1 in both the S and F regions, for the values of I indicated and the same angles as in Fig. 2.

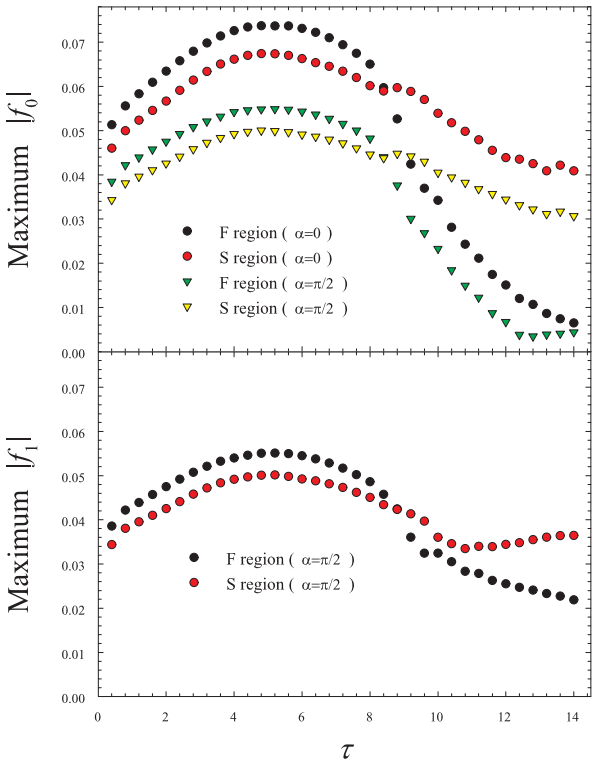

FIG. 4: Maximum absolute values of f_0 and f_1 (see text) as a function of dimensionless time τ at $I = 1$. In the top panel we consider f_0 at both $\alpha = 0$ and $\alpha = \pi/2$ while in the bottom panel we consider f_1 at $\alpha = \pi/2$.

On the F side, both amplitudes peak very near the interface and then decay in an oscillatory manner, reminiscent of the behavior of the usual pair amplitude. Although the height of the first peak does not depend strongly on I, the subsequent decay in the F material is faster for larger values of I. This can be attributed to a decreased overall proximity effect: here we have assumed that at $I = 0$ there would be no mismatch between the Fermi surface wavevectors of the two materials, implying that as I increases the mismatch between either the up or the down Fermi wavevectors $k_\uparrow$ and $k_\downarrow$, on the F side, and that in the S side increases. The location of this first peak depends very clearly on I, its distance to the interface decreasing as approximately $1/I$ consistent with the general rule that the oscillatory spatial dependences on the F side are determined by the inverse of $k_\uparrow - k_\downarrow$. The height of the first peak depends strongly on time and is maximum at times τ of about 2π. It is quite obvious that at intermediate values of I the penetration of the triplet correlation into the F material is rather long ranged.

On the superconducting side the behavior is quite different: the triplet correlations penetrate into the S material over a distance that rather quickly reaches two correlation lengths and then of course saturates at the sample size, without signs of decaying in time at these length

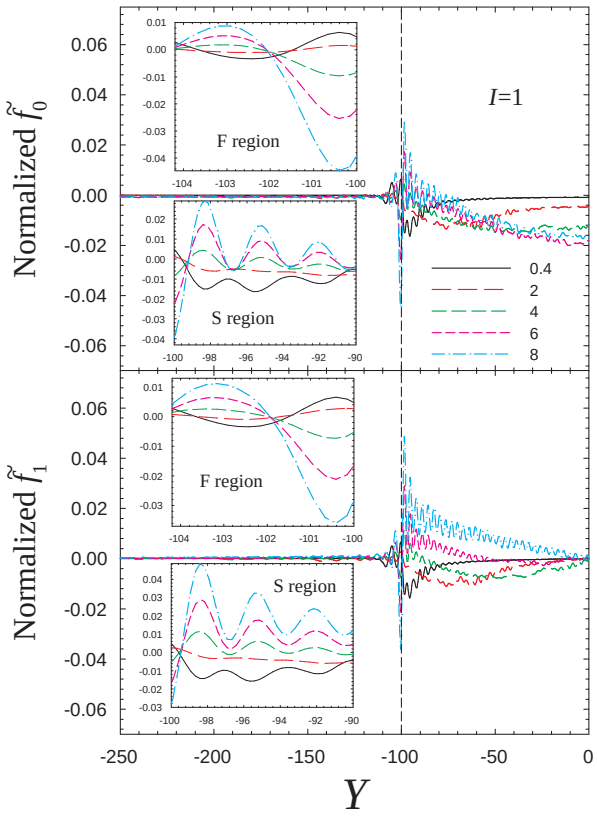

FIG. 5: Imaginary parts, $\tilde{f}_0(y,t)$ and $\tilde{f}_1(y,t)$ of the complex triplet amplitudes $\mathbf{f_0}(y,t)$ and $\mathbf{f_1}(y,t)$. These quantities are normalized and plotted exactly as their corresponding real parts are in Fig. 2, except that here we consider only the $I = 1$ case, and both plots are for $\alpha = \pi/2$. As in Fig. 2 the main plot shows the behavior over an extended region. There are now two insets to each main plot, each showing the detailed behavior near the interface itself, on either the S or F side.

scales. Furthermore this effect now increases sharply with I and is maximal in the half metallic case. Thus, the magnets act as sources, so to speak, of triplet correlations that enter the S material and this effect is stronger when I is larger.

It is instructive to extract characteristic penetration lengths ℓ_i from the above data using the definition,

$$\ell_i = \frac{\int dy |f_i(y,t)|}{\max |f_i(y,t)|}, \quad i = 0, 1, \tag{3.1}$$

where the integration is either over the S or the F region. In Fig. 3, the top two panels show the penetration lengths for the F material, at three values of I and the same values of α as for Fig. 2. The results are very similar whether they are calculated from the results for f_0 or from those for f_1. The penetration length at constant time decreases with I as already noted and shows signs of saturating with time at a value which for $I = 0.25$ approaches that of the superconducting coherence length. On the S side (bottom panels) the situation is very different: the results for f_0 and f_1 are now clearly dissimilar with the penetration length for the former quantity being (for cases shown here) the larger one. This arises from the geometry and magnetization projections of each F layer on the x axis, which are in opposite directions, forcing the triplet f_1 to possess a node at the center of the trilayer. No such requirement exists for f_0, as it is spatially symmetric. Except for the case of f_1 at $I = 1$, we see no sign of saturation. In fact, the maximum value of τ displayed here corresponds to the case in which the entire intrinsically singlet superconductor layer, two coherence lengths thick and sandwiched between two magnets, is wholly pervaded by induced triplet correlations.

It is also of interest to consider the variation of the spatial maximum values of $f_0(y,t)$ and $f_1(y,t)$ with time. In Fig. 4 we show, for each time, the largest value of these quantities, which typically is attained near the interface, in either the F or S regions. By "maximum" value we mean the maximum of $|f_0|$ and $|f_1|$, not to be confused with the absolute value of the complex quantities $|\mathbf{f_0}|$ or $|\mathbf{f_1}|$. In this figure, the magnets are half metallic, $I = 1$. In the top panel, we plot the results for f_0 at both $\alpha = 0$ and $\alpha = \pi/2$. We see that at earlier times, the value $f_0(y,t)$ at its peak just inside the F region (see Fig. 2, bottom left panel) exceeds the maximum value of this quantity in S. At longer times, however, there is a crossover as the size of the peaks in F decreases rather sharply, as explained above, while the size of the amplitude in S decreases only slowly, as the triplet correlations fill the S layer. It is apparent from careful examination of the $I < 1$ panels in Fig. 2, that this crossover does not occur for smaller values of I except possibly on a time scale much longer than that considered here. In the bottom panel, we present a similar study of f_1, this time of course only at $\alpha = \pi/2$ since this quantity vanishes identically for collinear magnetizations. The results are clearly very similar except that the results in the F region appear to saturate and do not decrease at long times. This is consistent with the earlier discussion where we saw that $|f_0|$ and $|f_1|$ overlap at $\alpha = \pi/2$, except at sufficiently long times. In all cases the maximum value of the quantity plotted crests near $\tau = 6$ in agreement with previous remarks.

All of the above results have been given in terms of the real parts, f_0 and f_1 of the complex amplitudes $\mathbf{f_0}$ and $\mathbf{f_1}$. The behavior of the corresponding imaginary parts is qualitatively very similar and thus we will present only two examples, in Fig. 5. We denote these imaginary parts by $\tilde{f}_0(y,t)$ and $\tilde{f}_1(y,t)$ respectively. In Fig. 5 we consider only the case $I = 1$ (compare with Fig. 2) and $\alpha = \pi/2$. As in Fig. 2 the main plots include an extended region near one of the interfaces and the insets are close views of the interface itself, in this case one of the insets shows a more detailed view of the S side. On the F side, the behavior is reminiscent to that of the real parts, except that the very prominent peak seen in the real parts right at the interface is absent for the imaginary parts. On the

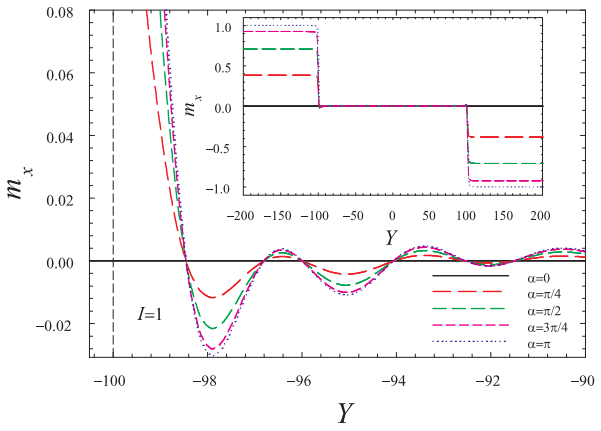

FIG. 6: Magnetic moment component m_x (see Eq. (2.21)), normalized as explained in the text, plotted vs position (at $I = 1$) for several values of α. The main plot shows the behavior near the interface (vertical dashed line), while the inset covers the whole sample.

S side, the sign is now initially negative and it changes to positive at τ of order unity. No such change was observed for the real parts. At longer times, the imaginary part of the triplet correlations also eventually penetrates several correlation lengths into the S sample, just as the real part does.

In the next two figures, we explore the reverse proximity effect (the spreading of the magnetism into the S layer) as a function of α. This is best done by considering separately the two components of the local magnetic moment vector. First, in Fig. 6 we consider the x component m_x (see Eq. (2.21)) normalized to the absolute value of its bulk value in a pure F material. The results in this figure are for half metallic magnets, ($I = 1$). In the main plot of the figure we display the value of m_x in the region very near an interface for several values of α. Of course, m_x vanishes at $\alpha = 0$. At other values of α it is large in the F material and it penetrates into S in an oscillatory way that is quite reminiscent of the corresponding penetration of the superconducting correlations into S. We see that the period of the spatial oscillations of the magnetization is independent of the angle α between the two F layer magnetizations. Another discernible feature is that m_x dampens out over relatively short length scales, consistent with past work.[34] The inset shows the overall behavior of m_x in the entire sample, demonstrating also the opposite signs between in the two magnets in accordance with Fig. 1.

Similarly, in Fig. 7 we display the z-component of m_z (see Eq. (2.20)), normalized in the same way as m_x, and for the same values of α but including now three different values of I. Again, the main plots display the behavior near the interface while the insets are for the entire sample. One can see here that the reverse proximity effect is very weak at small I and largest in the half metallic

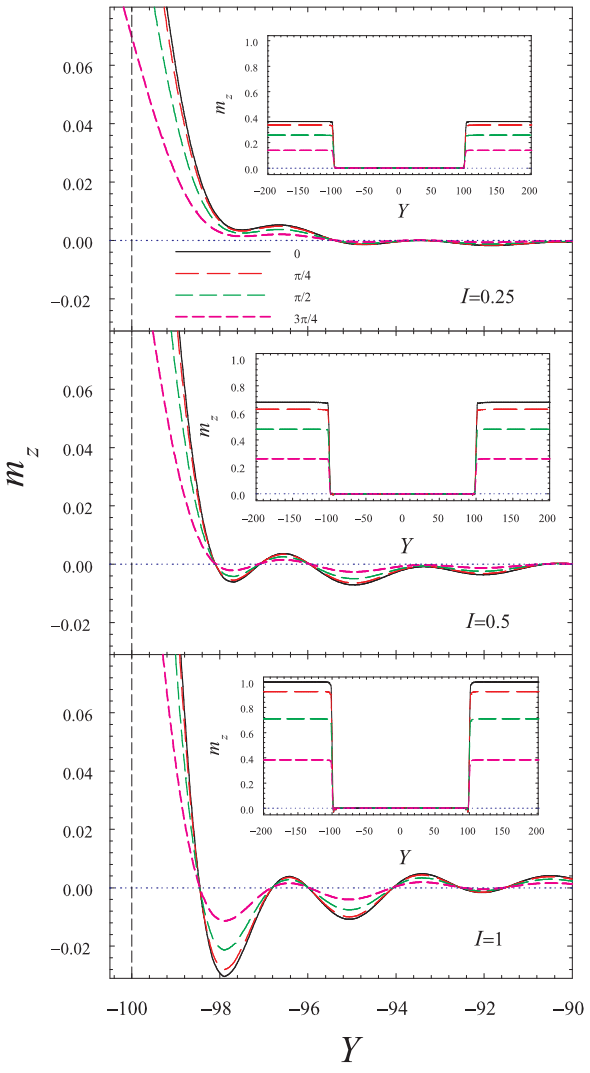

FIG. 7: Normalized (see text) magnetic moment component m_z (Eq. (2.20)) plotted vs. dimensionless position for three values of I. Again, the main plot is the behavior near the interface, while the insets cover the whole sample. It is evident that m_z points in the same direction for both magnets

case. The magnetic moment oscillates in the superconductor with a period that is independent of the direction and magnitude of the mutual magnetization in the F layers. The observed trends in m_z hold also for the m_x component.

We next study the energy dependence of the single particle quasiparticle spectrum by considering the local density of states (local DOS), $N(y, \epsilon)$, as defined in Eqn. (2.22). In Fig. 8 we consider the local DOS, integrated either over either the entire S or the entire F region, and normalized to its bulk value on a sample of

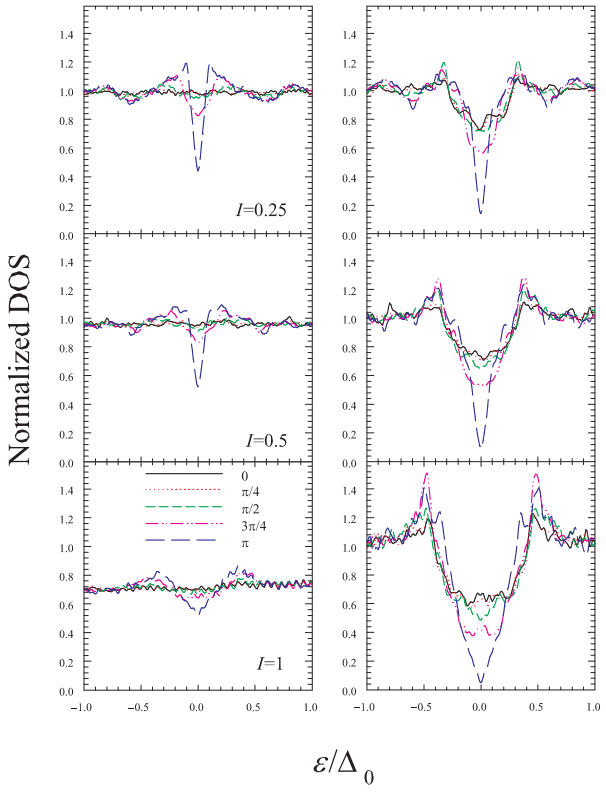

FIG. 8: Normalized local DOS from Eq. (2.22) integrated over (see text) over either the F region (left panels) or the S region (right panels) for three values of I and several relative magnetization orientations. The temperature is at $T = 0.01T_c$.

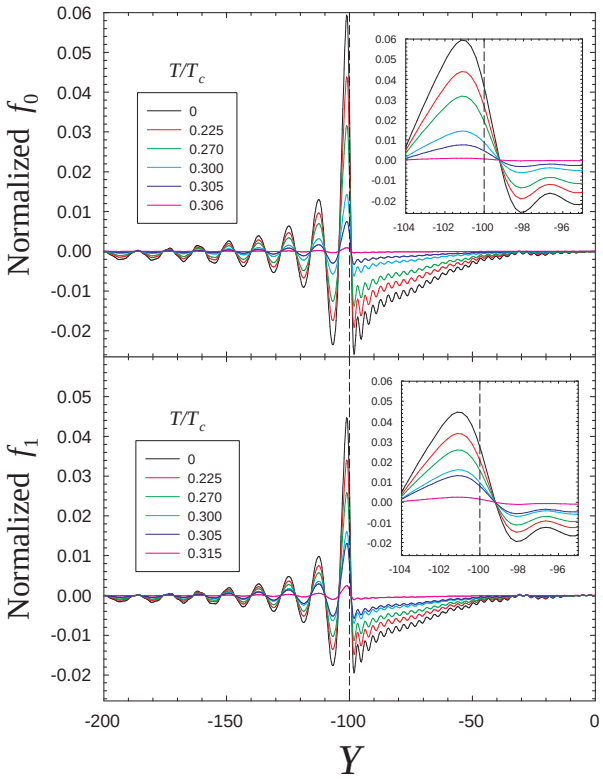

FIG. 9: Temperature and position dependence of f_0 and f_1 at $I = 0.5$ and $\tau = 4$. In the top panel $\alpha = 0$ and in the bottom panel $\alpha = \pi/2$. The values of T/T_c, where T_c is the transition temperature of bulk S, are indicated. The main plots show a rather wide region near the interface (vertical dashed line) and the insets focus on the region very near the interface.

the S material in its normal (non-superconducting) state. The results are displayed for three values of I and several values of α. The results reflect and confirm what we already have found out from analyzing the triplet amplitudes. On the F side, the proximity effect increases the correlations somewhat with α, as a reduction in quasiparticle states emerges for low energies due to increased correlations as the relative magnetizations become increasingly antiparallel. As I increases, the proximity effects weaken. Indeed, at $I = 1$ the DOS is nearly flat except at the larger values of α, suggesting that in the absence of a down spin band there may be a contribution from a possible triplet presence. On the superconducting side, the situation is somewhat different: the results never approach a limit where the local DOS would look similar to that of a bulk superconductor. Even at $I = 1$, there is never a gap and even when that situation is approached at larger α, when the magnetizations in the two F layers are antiparallel, the shape of the DOS curve does not resemble the signature bulk superconductor result. The profound difference between the parallel ($\alpha = 0$) and antiparallel ($\alpha = \pi$) cases is consistent in every respect with that previously[9] found.

The above results were all obtained in the low temperature limit. In the remaining figures we consider the

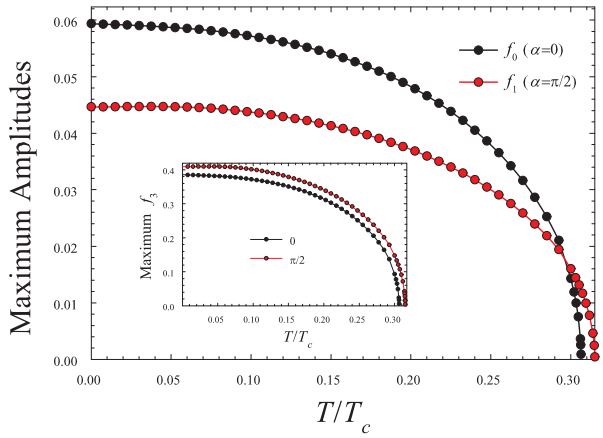

FIG. 10: The maximum values of the real parts of the triplet amplitudes at $I = 0.5$ and $\tau = 4$, as a function of temperature and the same values of α as in Fig. 9. The inset shows the corresponding peak values of the ordinary singlet amplitude, $f_3 \equiv \Delta(y)/g$ (Eq. (2.9)).

temperature dependence. In Fig. 9 we plot directly the spatial behavior of f_0 and f_1 over a broad range of temperatures. As in previous figures for the triplet amplitudes, the main plot shows the behavior over a relatively extended region of the sample and the insets magnify the region near interface. In both cases we have taken $I = 0.5$ and $\tau = 4$ while $\alpha = 0$ for f_0 and $\alpha = \pi/2$ for f_1. It can be inferred that at low T the temperature dependence of the triplet amplitudes is weak, while as T increases, the closer spacing in temperatures shown suggest that the correlations become destroyed at a much more rapid rate. In comparing the two panels, it is seen that for much of the temperature range, $|f_0| > |f_1|$, but at higher temperatures ($T \gtrsim 0.3T_c$), f_1 becomes the larger of the two. The temperature dependence of the characteristic penetration depths is weak. These observations are further exemplified in Fig. 10, where the peak values of $|f_0|$ and $|f_1|$ (also at $\tau = 4$) are shown as a function of T. These quantities are determined by calculating $\max\{f_0(y,T)\}$ and $\max\{f_1(y,T)\}$ throughout the structure for a given temperature. The inset depicts the corresponding peak values of the ordinary self- consistent equal-time singlet amplitude $f_3(y) \equiv \Delta(y)/g$, (see Eq. (2.9)). For both the triplet and singlet behavior, there is a strong dependence on T as the temperature approaches the system's transition temperature, which is about $0.32T_c$ for our system. Technically, the determination of the self consistent amplitudes is more difficult at higher T, when the number of iterations is in principle much higher. This increase in computational time can be reduced by up to an order of magnitude by taking as the initial spatial pair potential at a given T the result for the previously obtained next lower temperature times a T dependent factor derived from the linearized Ginzburg-Landau theory[32].

In accordance with what we have just seen, it is a natural extension to study how thermal effects might destroy the spatial characteristics of singlet correlations throughout the structure. In Fig. 11, we therefore display f_3 as a function of Y, for several temperatures, and in which the relative magnetizations are collinear ($\alpha = 0$) and at right angles ($\alpha = \pi/2$). Remarkably, one can see that the temperature dependence of the triplet components is somewhat weaker that that of the standard singlet amplitude. One can also clearly see that, as indicated above, the penetration of the triplet amplitudes into the F material over a length scale that is clearly much longer than that of the singlet amplitude. This is again a strong indication that experimental tunneling results indicating long ranged penetration effects in F/S structures are indeed evidence for induced triplet correlations.

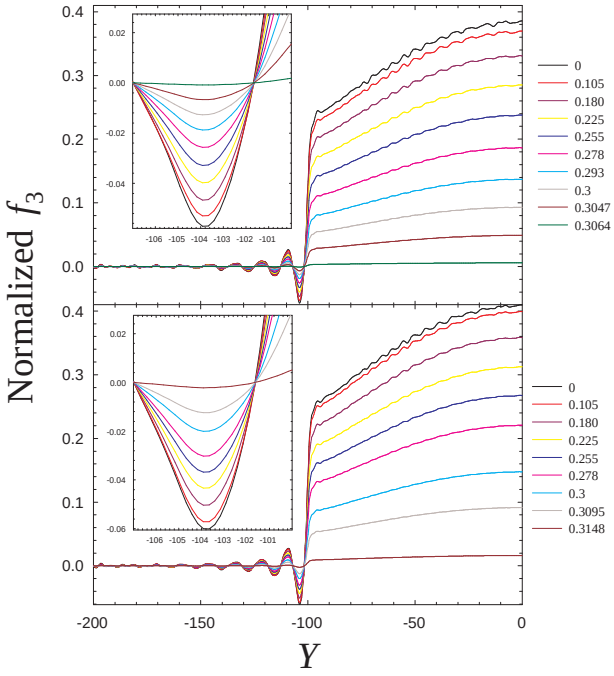

FIG. 11: Temperature and position dependence of the ordinary singlet pair amplitude (or $\Delta(y)/g$)), normalized to its value in bulk S material, for moderate magnetic strength, $I = 0.5$. Top panel: the magnetizations are parallel ($\alpha = 0$). Bottom panel: the magnetizations are perpendicular ($\alpha = \pi/2$).

IV. CONCLUSIONS

In this paper, we have presented a detailed study of induced time dependent (odd in time) triplet pairing correlations in clean planar FSF junctions consisting of an ordinary s-wave superconductor sandwiched between two relatively thick ferromagnets whose magnetizations are misoriented with respect to each other by an angle α. Our microscopic formalism allowed us to investigate cases involving strong magnets, as well as atomic scale phenomenon, two things not possible in the widely used quasiclassical approaches. We have obtained results as a function of α, time, the strength I of the ferromagnets, and the temperature. We have presented results for the spatial behavior of the time-dependent triplet pair amplitudes, f_0 and f_1, and for the corresponding penetration lengths extracted from them. We have found that these triplet correlations are indeed induced via the proximity effect, that they completely pervade even a superconductor several coherence lengths thick, and also substantially penetrate the ferromagnetic layers. These results have clear implications for the experimental work in which long range proximity effects in SF nanostructures have been reported, effects that have been speculated to be due to the existence of some kind of triplet pairing. Our calculations, in which the time dependence is studied from the Heisenberg picture, emphasize the need for full self-consistency of the solutions, without which we find that the Pauli principle is violated.

We have also considered the reverse proximity effect, which is of particular interest in this case due to the presence of two components of the magnetization, and we also have given results for the experimentally measurable lo-

cal density of states, which revealed clear subgap energy signatures as a function of α and I. We have studied the temperature dependence of the triplet amplitudes (as well as the ordinary singlet amplitude) and found that the temperature dependence of the penetration depths associated with these triplet amplitudes is weak: these lengths remain large all the way up to the vicinity of the transition temperature of the system. This bodes well for further experimental observations and verification in these clean systems.

Acknowledgments

This project is funded in part by the Office of Naval Research (ONR) In-House Laboratory Independent Research (ILIR) Program and by a grant of HPC resources from the Arctic Region Supercomputing Center at the University of Alaska Fairbanks as part of the Department of Defense High Performance Computing Modernization Program.

* Electronic address: klaus.halterman@navy.mil
† Electronic address: otvalls@umn.edu; Also at Minnesota Supercomputer Institute, University of Minnesota, Minneapolis, Minnesota 55455
‡ Electronic address: barsic@physics.umn.edu; Current address: Areté Associates, 1550 Crystal Dr., Arlington, Virginia 22202

[1] D.D. Osheroff, R.C. Richardson and D.M. Lee, Phys. Rev. Lett. bf 28, 885 (1972).
[2] V.L. Berezinskii, JETP Lett. **20**, 287, (1974).
[3] Aurel Bulgac, Michael McNeil Forbes, and Achim Schwenk, Phys. Rev. Lett. **97**, 020402 (2006).
[4] Igor Žutić, Jaroslav Fabian, S. Das Sarma, Rev. Mod. Phys. **76**, 323 (2004).
[5] J. Y. Gu, C.-Y. You, J. S. Jiang, J. Pearson, Ya. B. Bazaliy, and S. D. Bader, Phys. Rev. Lett. **89**, 267001 (2002).
[6] I. C. Moraru, W. P. Pratt, N. O. Birge, Phys. Rev. Lett. **96**, 037004 (2006).
[7] C. Bell, S. Turşucu, and J. Aarts, Phys. Rev. B **74**, 214520 (2006).
[8] C. Visani, V. Peña, J. Garcia-Barriocanal, D. Arias, Z. Sefrioui, C. Leon, J. Santamaria, N.M. Nemes, M. Garcia-Hernandez, J.L. Martinez, S.G.E. te Velthuis and A. Hoffmann, Phys. Rev. B **75**, 054501 (2007).
[9] K. Halterman and O.T. Valls, Phys. Rev. B **72**, 060514(R) (2005).
[10] P. G. de Gennes, Phys. Lett. **23**, 10 (1966).
[11] L.R. Tagirov, Phys. Rev. Lett. **83**, 2058 (1999).
[12] A.I. Buzdin, A.V. Vdyayev, and N.V. Ryzhanova, Europhys. Lett. **48**, 686 (1999).
[13] V. Peña, Z. Sefrioui, D. Arias, C. Leon, J. Santamaria, M. Varela, S. J. Pennycook, J. L. Martinez, Phys. Rev. B **69**, 224502 (2004).
[14] K. D. Nelson, Z. Q. Mao, Y. Maeno, Y. Liu, Science **306**, 1151 (2004).
[15] V.N. Krivoruchko and V. Yu. Taernkov Phys. Rev. B **75**, 214508 (2007).
[16] R. S. Keizer, S. T. B. Goennenwein, T. M. Klapwijk, G. Miao, G. Xiao, A. Gupta, *Nature* **439**, 825, (2006).
[17] F.S. Bergeret, A.F Volkov, and K.B. Efetov, Rev. Mod. Phys. **77**, 1321 (2005).
[18] K. Halterman, P.H. Barsic, and O.T. Valls Phys. Rev. Lett. **99**, 127002 (2007).
[19] F.S. Bergeret, A.F Volkov, and K.B. Efetov, Phys. Rev. Lett. **86**, 3140 (2001).
[20] F. S. Bergeret, A. F. Volkov, and K. B. Efetov, Phys. Rev. B **68**, 064513 (2003).
[21] T. Champel and M. Eschrig, Phys. Rev. B **72**, 054523 (2005).
[22] Ya. V. Fominov, A. F. Volkov, and K. B. Efetov Phys. Rev. B **75**, 104509 (2007).
[23] V. Braude and Yu. V. Nazarov Phys. Rev. Lett. **98**, 077003 (2007).
[24] M. Houzet and A.I. Buzdin Phys. Rev. B **76**, 060504(R) (2007).
[25] Ya. V. Fominov, A. A. Golubov, and M. Yu. Kupriyanov, JETP Lett. **77**, 510 (2003).
[26] T. Löfwander, T. Champel, J. Durst, and M. Eschrig, Phys. Rev. Lett. **95**, 187003 (2005).
[27] A.I. Buzdin, Rev. Mod. Phys. **77**, 935 (2005).
[28] Y. Asano, Y. Sawa, Y. Tanaka, and A. Golubov, Phys. Rev. B **76**, 224525 (2007).
[29] T. Yokoyama, Y. Tanaka, and A.A. Golubov, Phys. Rev. B **75**, 134510 (2007).
[30] Y. Tanaka, Y. Tanuma, and A. A. Golubov, Phys. Rev. B **76**, 054522 (2007).
[31] J. Linder and A. Sudbø, Phys. Rev. B **75**, 134509 (2007).
[32] P.G. de Gennes, *Superconductivity of Metals and Alloys*, (Addison-Wesley, Reading, MA, 1989).
[33] J. B. Ketterson and S. N. Song, *Superconductivity*, (Cambridge University Press, Cambridge, UK 1999), p. 286.
[34] K. Halterman and O.T. Valls, Phys. Rev. B **69**, 014517 (2004).
[35] K. Halterman and O.T. Valls, Phys. Rev. B **70**, 104516 (2004).